Reach of Fermilab Tevatron upgrades for SU(5) supergravity models with nonuniversal gaugino masses

Greg Anderson,[1] Howard Baer,[2] Chih-Hao Chen,[2] Pamela Quintana,[2] and Xerxes Tata[3]

[1]*Department of Physics, Northwestern University, Evanston Illinois 60208*

[2]*Department of Physics, Florida State University, Tallahassee, Florida 32306*

[3]*Department of Physics and Astronomy, University of Hawaii, Honolulu, Hawaii 96822*

We explore the reach of luminosity upgrades of the Fermilab Tevatron collider for $SU(5)$ supergravity models in which non-universal GUT-scale gaugino masses arise via a vacuum expectation value for the auxiliary component of a superfield that transforms as a **24, 75 or 200** dimensional representation of $SU(5)$. This results in a different pattern of sparticle masses and mixing angles from what is expected in the minimal supergravity (MSUGRA) model with universal GUT scale gaugino masses. We find that the resulting signal cross sections, and hence the reach of the Tevatron, are sensitive to the gaugino masses at the GUT scale. In the **24** model, the large splitting amongst the two lightest neutralinos leads to SUSY events containing many isolated leptons, including events with a real leptonic Z boson plus jets plus missing energy signal which is visible over much of parameter space. In contrast, in the **75** and **200** models, the reach via leptonic SUSY signals is greatly reduced relative to MSUGRA, and the signal is usually visible only via the canonical $\not{E}_T$ + jets channel.

PACS number(s): 14.80.Ly, 11.30.Pb, 13.85.Qk

I. INTRODUCTION

The minimal supergravity (MSUGRA) model [1] provides a well-motivated and economical framework in which to embed the minimal supersymmetric standard model [2], (MSSM). In MSUGRA, supersymmetry (SUSY) is broken in a hidden sector, and SUSY breaking is communicated to the visible sector MSSM fields via interactions of gravitational strength. Motivated by the apparently successful gauge coupling unification in the MSSM, it is usually assumed that this leads to a common value m_0 for all scalars, a common mass $m_{1/2}$ for all gauginos, and a common trilinear SUSY breaking term A_0 at the scale $M_{\rm GUT} \simeq 2 \times 10^{16}$ GeV. The soft SUSY breaking terms, the gauge and Yukawa couplings and the supersymmetric μ term are all then evolved from $M_{\rm GUT}$ to some scale $M \simeq M_{weak}$ using renormalization group equations (RGE's). Electroweak symmetry is broken radiatively due to the large top quark Yukawa coupling. The resulting weak scale spectrum of superpartners and their couplings can then be derived in terms of four continuous plus one discrete parameters

$$m_0, \quad m_{1/2}, \quad A_0, \quad \tan\beta \quad \text{and} \quad \text{sgn}(\mu), \quad (1.1)$$

in addition to the usual parameters of the standard model.

In studies of MSUGRA and other supersymmetric extensions of the standard model based on gauge-unification and the gravitational mediation of supersymmetry-breaking, it is often assumed (as discussed above) that the unification of gauge interactions implies a similar unification of gaugino masses at the scale of gauge-coupling unification. However, gravitationally mediated supersymmetry breaking may lead to non-universal gaugino masses even in the presence of gauge coupling unification. We present a class of models which contain non-universal gaugino masses, discuss their experimental signatures at the Fermilab Tevatron, and contrast those signatures with those of MSUGRA. The models

we discuss represent equally predictive alternatives to the canonical universal gaugino mass scenario.

If gravity is the messenger which communicates supersymmetry breaking from the hidden to the visible sector, supersymmetry breaking mass terms for gauginos can arise from higher dimensional interactions which couple a chiral superfield to the supersymmetric field strength [3]. These interactions arise from the locally supersymmetric gauge field strength interactions:

$$\mathcal{L} \supset \int d^4\theta E(R^{-1}f_{ab}W^aW^b + \text{H.c.}) \quad (1.2)$$

with a gauge kinetic function $f_{AB} = \delta_{AB} + \Phi_{AB}/M_{Planck} + \dots$. The fields Φ_{AB} transform as left handed chiral superfields under supersymmetry transformations, and as the symmetric product of two adjoints under gauge symmetries. The lowest order contribution to gaugino masses arising from the interaction above comes from a dimension five operator:

$$\mathcal{L} \supset \int d^2\theta W^aW^b \frac{\Phi_{ab}}{M_{\rm Planck}} + \text{H.c.} \supset \frac{\langle F_\Phi \rangle_{ab}}{M_{\rm Planck}} \lambda^a \lambda^b + \dots, \quad (1.3)$$

where the $\lambda^{a,b}$ are the gaugino fields, and F_Φ is the auxiliary field component of Φ.

TABLE I. Relative gaugino masses at $M_{\rm GUT}$ and M_Z in the four possible F_Φ irreducible representations.

F_Φ	$M_{\rm GUT}$			M_Z		
	M_3	M_2	M_1	M_3	M_2	M_1
1	1	1	1	~6	~2	~1
24	2	-3	-1	~12	~-6	~-1
75	1	3	-5	~6	~6	~-5
200	1	2	10	~6	~4	~10
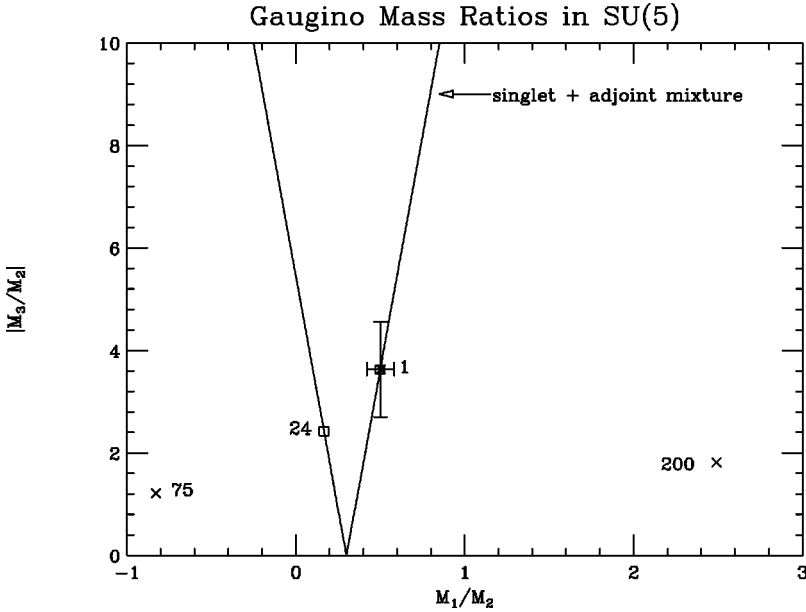
FIG. 1. Gaugino mass ratios for the four special cases where the field Φ transforms as the **1**, **24**, **75** or **200** dimensional representation of $SU(5)$, or as an arbitrary linear combination of the singlet and adjoint representations (solid line).

In conventional models of supersymmetry breaking, the fields F_Φ which break supersymmetry are treated as gauge singlets. However, in principle, the chiral superfield which communicates supersymmetry breaking to the gaugino fields can lie in any representation found in the symmetric product of the adjoint. Non gauge singlet vacuum expectation values for the supersymmetry preserving component of Φ_{AB} have been considered previously [4,5] for their perturbative effect on gauge coupling unification and also for their effect on gaugino masses [4,6–8]. Here we consider the effect of supersymmetry breaking vacuum expectation values of Φ_{AB} which lead to maximally predictive gaugino masses. In the context of $SU(5)$ grand unification, F_Φ belongs to an $SU(5)$ irreducible representation which appears in the symmetric product of two adjoints:

$$(\mathbf{24} \times \mathbf{24})_{\text{symmetric}} = \mathbf{1} \oplus \mathbf{24} \oplus \mathbf{75} \oplus \mathbf{200}, \qquad (1.4)$$

where only **1** yields universal masses. Only the component of F_Φ that is ''neutral'' with respect to the SM gauge group should acquire a vaccum expectation value (VEV), $\langle F_\Phi \rangle_{ab} = c_a \delta_{ab}$, with c_a then determining the relative magnitude of the gaugino masses at M_{GUT}. The relations amongst the various grand unified theory (GUT) scale gaugino masses have been worked out, e.g., in Ref. [8]. The relative GUT scale $SU(3)$, $SU(2)$, and $U(1)$ gaugino masses M_3, M_2, and M_1 are listed in Table I along with the approximate masses after RGE evolution to $Q \sim M_Z$. Here, motivated by the measured values of the gauge couplings at the CERN e^+e^- collider LEP, we assume that the VEV of the scalar component of Φ is neglible. In principle, as shown in Fig. 1, an arbitrary linear combination of the above irreducible representations is also allowed. We consider the implications of models where the dominant contribution to gaugino masses arises from a single irreducible

representation.[1] Each of the three non-singlet models is as predictive as the canonical singlet case, and all are compatible with the unification of gauge couplings. These scenarios represent the predictive subset of the more general case [7] of an arbitrary superposition of these representations,[2] the most interesting being a superposition of gauge singlet and adjoint fields.

As we discuss in Sec. III, signals of supersymmetry—and hence the reach of the Tevatron—is sensitive to the structure of the gaugino masses as the GUT scale. The reach of the Fermilab Tevatron collider for MSUGRA models with universal gaugino masses has been worked out for both low [9–12] as well as high [13] values of the parameter $\tan\beta$. For low values of $\tan\beta$ and high integrated luminosity, the clean trilepton signal (referred to as C3L) [14] from $\tilde{W}_1 \tilde{Z}_2 \to l'\bar{l}l + \not{E}_T$ usually offers the best prospect for a SUSY discovery. For parts of parameter space, a SUSY signal might be found in several different channels. For large $\tan\beta$, discovery via the C3L signal becomes increasingly difficult because sparticle decays to τ-leptons and b-quarks becomes

---

[1]From the point of view of the theory below the GUT scale, we may consider the use of the large representations listed in Eq. (1.4) as a calculational convenience. Only the $SU(3) \times SU(2) \times U(1)$ singlet components of these representations are relevant to our discussion. The remaining states may obtain masses which are heavy compared to M_{GUT}. Any relic of a large GUT representation which survives below the GUT scale and has a non-vanishing coupling to the supersymmetric field strength, must lie in the symmetric product the adjoint representations of the unified group, and further this relic must be a $SU(3) \times SU(2) \times U(1)$ singlet. For the unification group $SU(5)$, the complete set of masses produced by relics from pure $SU(5)$ representations are those listed in Table I.

[2]In Ref. [6], a specific linear combination was fixed by the additional assumption of the vanishing of this contribution to leptoquark gaugino masses.
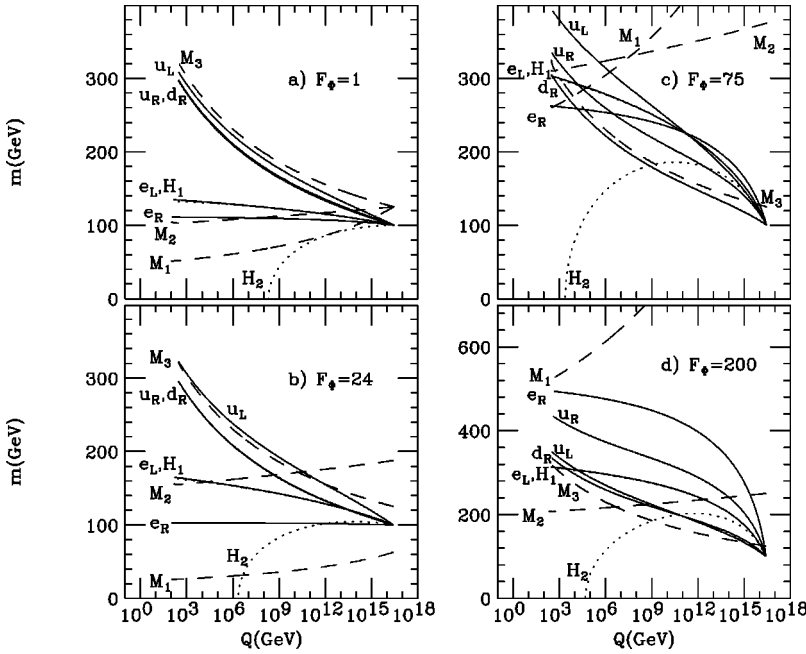
FIG. 2. A plot of the evolution of soft SUSY breaking parameters versus renormalization scale Q from M_{GUT} to M_{weak} for SUGRA model parameters $m_0 = 100$ GeV, $M_3^0 = 125$ GeV, $A_0 = 0$, $\tan\beta = 5$, and $\mu > 0$, for the (a) $F_\Phi \sim 1$, (b) $F_\Phi \sim 24$, (c) $F_\Phi \sim 75$, and (d) $F_\Phi \sim 200$ models. In frame (b), M_1 and M_2 are negative, while in frame (c), M_1 is negative; the curves then show the magnitudes of these parameters. We take $m_t = 175$ GeV. Notice the different scale in frame (d).

enhanced relative to decays to e's and μ's. Recent studies [15–17] of the trilepton signal have shown that the range of parameters over which the signal is observable may be extended by the use of softer cuts on the leptons compared to cuts used in earlier studies: in this case there are important new SM background contributions from $W^*\gamma^*$ and W^*Z^* production that have to be incorporated into the analysis. The largest reach is then obtained via the inclusive trilepton channel without a veto on events with jets.

We should add that we do not specially advocate any particular representation for $\langle F_\Phi \rangle$ on theoretical grounds. Our main motivation is to examine the sensitivity of the various signals via which SUSY might manifest itself at future runs of the Tevatron to changes in the underlying framework. It is especially important to do so when assessing the search capabilities of future facilities, particularly because we do not as yet have a dynamical understanding of SUSY breaking, which can affect the phenomenology via the pattern of sparticle masses and mixing angles.

With this in mind, the event generator ISAJET [18] (versions ≥ 7.37) has been upgraded to accommodate SUGRA models with various non-universal soft SUSY breaking terms. In this study, we use ISAJET to simulate models with non-universal gaugino mass parameters at the scale M_X assuming universality of other parameters. The model parameter space used in this paper thus corresponds to

$$m_0, \quad M_3^0, \quad A_0, \quad \tan\beta \quad \text{and} \quad \text{sgn}(\mu), \quad (1.5)$$

where M_i^0 is the $SU(i)$ gaugino mass at scale $Q = M_{GUT}$. M_2^0 and M_1^0 can then be calculated in terms of M_3^0 according to Table I. ISAJET calculates an iterative solution to the 26 RGEs, and imposes the radiative electroweak symmetry breaking constraint. This determines all sparticle masses and mixings. Next, branching fractions for all sparticles, particles and Higgs bosons are calculated. Supersymmetric particle production events can be generated for all possible $2 \rightarrow 2$

SUSY hard scattering subprocesses. Sparticle production is followed by initial and final state parton showers, cascade decays, hadronization and underlying event simulation. Thus, specific assumptions about soft SUSY breaking terms that are motivated by GUT or string scale physics can be directly tested at collider experiments.

In this paper, we explore the consequences of non-universal gaugino masses for $SU(5)$ SUGRA GUT models for the Fermilab Tevatron collider and its planned upgrades. Our goals are several.

We wish to establish the capability of the Tevatron and its upgrades to discover or rule out SUSY within the context of models alternative to MSUGRA. The set of models we examine maintain many of the attractive features of generic SUGRA models, while exhibiting radically different sparticle mass spectra and mixing angles from the commonly examined models which assume universality.

We want to see if this class of models examined can be distinguished one from another. If certain SUSY signals are observed, the answer appears to be yes for a limited region of model parameter space.

Are there any new signals for SUSY that can occur within the context of non-standard SUSY models? We will see that in the $F_\Phi \sim \mathbf{24}$ model, there is a large range of parameter space that leads to signal events containing real leptonic Z bosons. These signals occur much more rarely in the MSUGRA model.

Non-universality of gaugino masses can also arise in other model contexts [19] including some string models [20]. Phenomenological consequences of O-II string models have been examined in Ref. [21].

In Sec. II, we outline features of the mass spectra that are consequences of the assumptions about the $SU(5)$ representation of the hidden sector field(s) Φ that can occur. In Sec. III, we outline the various types of signals that could occur for SUSY models, and our signal and background event gen-
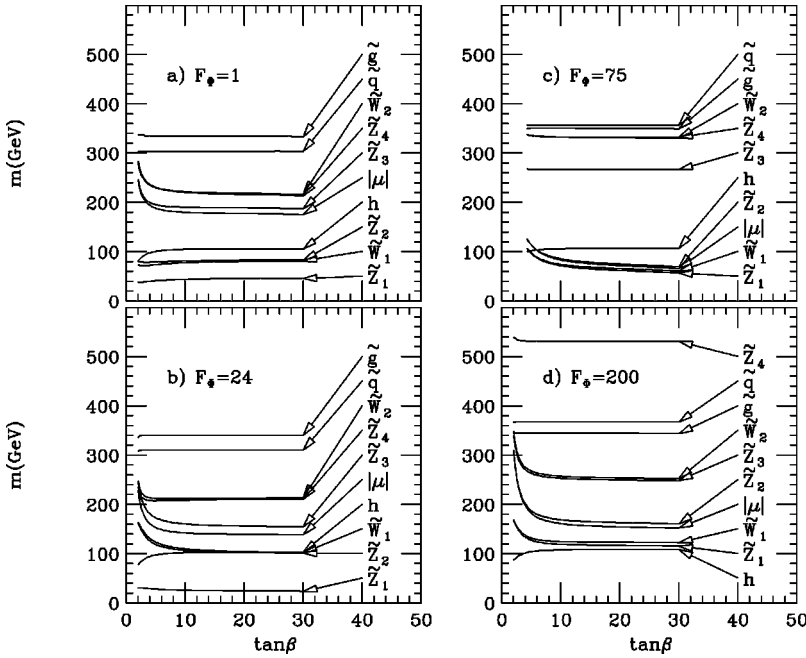
FIG. 3. A plot of various physical sparticle masses and the magnitude of the μ parameter (positive in this case) versus $\tan\beta$ for SUGRA model parameters $m_0 = 100$ GeV, $M_3^0 = 125$ GeV, $A_0 = 0$, and $\mu > 0$, for the (a) $F_\Phi \sim 1$, (b) $F_\Phi \sim 24$, (c) $F_\Phi \sim 75$, and (d) $F_\Phi \sim 200$ models. The squark mass is averaged over the first two generations.

erator calculations. In Sec. IV, we present results of the reach of Tevatron upgrade options for each of the four models considered. In Sec. V, we present a summary and some conclusions.

II. SPARTICLE MASSES FOR SUGRA MODELS

We begin by illustrating the evolution of the magnitude of soft SUSY breaking masses versus scale Q in Fig. 2 for the four model choices (a) $F_\Phi \sim 1$, (b) $F_\Phi \sim 24$, (c) $F_\Phi \sim 75$, and (d) $F_\Phi \sim 200$. We take $m_0 = 100$ GeV, $M_3^0 = 125$ GeV, $A_0 = 0$, $\tan\beta = 5$, and $\mu > 0$. Throughout this paper, we take $m_t = 175$ GeV.

The gaugino masses are denoted by dashed lines, while Higgs masses are denoted by dotted lines and squark and slepton masses are denoted by solid lines. For the usual MSUGRA case illustrated in Fig. 2(a), the gaugino masses evolve from a common GUT scale value. For the $F_\Phi \sim 24$ model in frame (b), the splitting in GUT scale gaugino masses shown in Table I leads to a large mass gap between M_1 and M_2 at the weak scale, and also a large mass gap between left and right sfermions. In case (c) for $F_\Phi \sim 75$, the large GUT scale splitting of gaugino masses leads to near gaugino mass degeneracy at the weak scale, and also similar masses for both squarks and sleptons. Finally, for case (d) with $F_\Phi \sim 200$, the large GUT scale splitting leads to $M_2, M_3 < M_1$ at the weak scale. In addition, the large GUT scale values of M_1 and M_2 cause the weak scale slepton masses to evolve to relatively high masses compared to the $F_\Phi \sim 1$ and 24 models, so that left sfermions are lighter than right sfermions; this is in contrast to usual expectations from models with universal gaugino masses. The $m_{H_2}^2$ mass parameter initially has an upward trajectory, but is ultimately evolved to negative values so that radiative electroweak

symmetry is just barely broken.

A variety of physical sparticle masses along with the magnitude of the weak scale μ parameter are shown versus $\tan\beta$ in Fig. 3 for the four model choices using the same parameters as in Fig. 2. Frame (a) shows the generic MSUGRA model spectrum for comparison with the models with non-universal gaugino masses. In frame (b), the large mass gap between $m_{\widetilde{W}_1}$ or $m_{\widetilde{Z}_2}$ and $m_{\widetilde{Z}_1}$ is apparent. This mass gap has important consequences for collider experiments: frequently it is so large that neutralino decays to real Z bosons are often allowed. Signatures involving real Z's could be a distinctive signature for models leading to large mass gaps between $\widetilde{Z}_2$ and $\widetilde{Z}_1$.

For the $F_\Phi \sim 75$ case in frame (c), there is almost no mass gap between $m_{\widetilde{W}_1}$ and $m_{\widetilde{Z}_1}$. For instance, for $\tan\beta = 5$, with the other parameters as in the figure, $m_{\widetilde{W}_1} - m_{\widetilde{Z}_1}$ is just[3] 0.5 GeV; this gap increases slightly with $\tan\beta$. (The smallness of this mass gap appears to be due to an accidental cancellation that occurs when $M_2/M_1 = -1.2$ but not when $M_2/M_1 = 1.2$.) The mass difference between $\widetilde{Z}_2$ and $\widetilde{Z}_1$ though larger (~ 18 GeV for $\tan\beta = 5$) is still considerably smaller than in the canonical MSUGRA case. In this case, decays of $\widetilde{Z}_2$ and certainly $\widetilde{W}_1$ will lead to very soft visible particles which will make detection of hard isolated leptons from cascade decays very difficult. In view of the very tiny mass difference between the chargino and $\widetilde{Z}_1$, the reader may legitimately wonder whether the chargino is sufficently long lived as to travel a substantial distance in the detector, thus leaving a track before decaying. We have checked,

---

[3]Radiative corrections, which have not been included here, could possibly be comparable and need to be included in a more refined simulation.
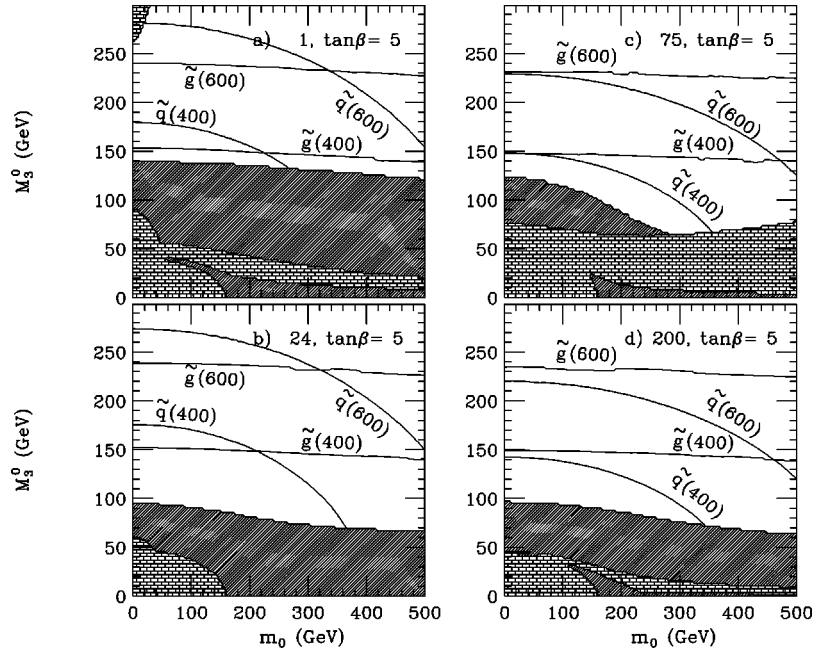
FIG. 4. A plot of gluino and squark mass contours in the m_0 vs M_3^0 plane for SUGRA model parameters $A_0=0$, $\tan\beta=5$, and $\mu>0$ for the (a) $F_\Phi\sim1$, (b) $F_\Phi\sim24$, (c) $F_\Phi\sim75$, and (d) $F_\Phi\sim200$ models. The squark mass is averaged over the first generation.

however,[4] that the lifetime of the chargino is $\mathcal{O}(10^{-11}$ s) so that this appears not to be the case.

For the $F_\Phi\sim\mathbf{200}$ model in frame (d), the $\widetilde{W}_1$-$\widetilde{Z}_1$ mass gap is just a few GeV, while $m_{\widetilde{Z}_2}-m_{\widetilde{Z}_1}$ is several tens of GeV. We have checked, however, that $\tau_{\widetilde{W}_1}\gtrsim10^{-15}$ seconds, so that it decays rapidly without an appreciably displaced vertex. In this case, the $\widetilde{Z}_4$ is mainly a bino, and is the heaviest of all the sparticles.

Aside from that alteration of the masses, the weak scale values of the gaugino masses in Table I also imply very different mixing patterns for the charginos and neutralinos as compared to the usual MSUGRA case. In contrast to the MSUGRA case, $|\mu|$ tends to be somewhat smaller than M_2, and the lighter neutralinos and $\widetilde{W}_1$ are dominantly Higgsino-like in the **75** and **200** cases. This impacts on the decays of sparticles, e.g. $\widetilde{Z}_2$ and sometimes also $\widetilde{W}_1$ production in cascade decays tends to be suppressed, while frequently heavier charginos and neutralinos are produced with large rates. The decay patterns of $\widetilde{W}_1$ and $\widetilde{Z}_2$ are also changed from usual MSUGRA expectation. This will reflect itself in changes in

expected rates for various event topologies as we will see later.

The different boundary condition for gaugino masses sometimes has a strong effect on other masses via the RGE. For instance, for the $F_\Phi\sim\mathbf{200}$ model shown in frame (d), the huge GUT scale value of $M_1=1250$ GeV causes right slepton and squark masses to evolve to large values so that in this case $m_{\tilde{e}_R}>m_{\tilde{q}}>m_{\tilde{e}_L}$. Another significant difference from the usual MSUGRA case is the large splittings between the masses of various squarks in the **75** and **200** cases. Indeed it is sometimes possible to have $m_{\tilde{q}_L}\gtrsim m_{\tilde{g}}\gtrsim m_{\tilde{q}_R}$, so that gluinos decay almost exclusively to right handed squarks. This, in turn, alters the cascade decay patterns from the usual expectation because the right handed squarks cannot decay into charginos and neutralinos with dominant $SU(2)$ components.

In Fig. 4, we show gluino and squark mass contours in the m_0 vs M_3^0 plane for $\tan\beta=5$, $A_0=0$, and $\mu>0$. The bricked regions are excluded by theoretical constraints: either electroweak symmetry is not broken appropriately [i.e. the calculated value of μ^2 is less than zero], or the lightest SUSY particle (LSP) is not the lightest neutralino, in contradiction with results from searches for stable cosmological relics. These regions are sensitive to the exact choice of m_t. The gray shaded regions are excluded by collider search experiments for SUSY particles, and are mainly formed from the LEP2 bound that $m_{\widetilde{W}_1}>85.5$ GeV [22,23]; the LEP2 bound from the non-observation of h plays a smaller role since for $\tan\beta=5$, m_h is usually not small. The chargino bounds used may actually be too stringent for the $F_\Phi\sim\mathbf{75}$ and **200** models where the $m_{\widetilde{W}_1}-m_{\widetilde{Z}_1}$ mass gap is small; for

---

[4]Because the mass gap is smaller than 1 GeV, it is not reasonable to compute the hadronic decay width of the chargino using ISAJET, which really computes the decay $\widetilde{W}_1\to q\bar{q}\widetilde{Z}_1$. Instead it is more reasonable to compute exclusive decays into 1,2, etc. pion states in association with $\widetilde{Z}_1$. We are grateful to M. Drees who has provided us a code to do so. For the $\tan\beta=5$ point discussed in the text, the lifetime using this code agrees with the ISAJET lifetime to within a factor 2. For the decay of $\widetilde{Z}_2$ for which the mass gap is ~20 GeV, the decays can, of course, be calculated using ISAJET.
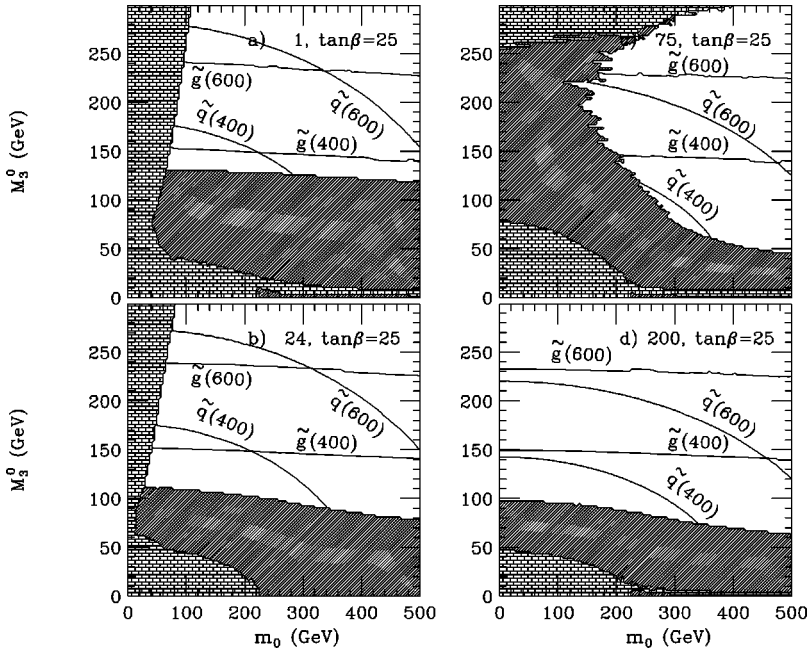
FIG. 5. Same as Fig. 4 except for $\tan\beta = 25$.

these cases, the LEP2 limits will have to be re-analyzed.[5] The gluino and squark mass contours are intended for comparison with the parameter space reach plots that will be presented in Sec. III of this paper. In Fig. 5, we show the same mass contours for $\tan\beta = 25$. In this case, the parameter space is much more restrictive. In particular, for the $F_\Phi \sim$ **75** model in frame (c), radiative electroweak symmetry breaking is difficult to achieve for large values of the parameter M_3^0. This is because in this case the gaugino masses M_1 and especially M_2 become quite large, off-setting the top quark Yukawa coupling constant which tends to drive $m_{H_2}^2$ to negative values in the renormalization group evolution.

III. EVENT SIMULATION AND REACH CALCULATIONS

In several previous studies [9–13], a variety of signal channels for the discovery of MSUGRA (with universal GUT scale gaugino masses) at the Tevatron were investigated, and the reach of the Tevatron Main Injector era (MI-integrated luminosity of 2 fb^{-1}) and TeV33 era (integrated luminosity of $\sim$25 fb^{-1}) were delineated in the parameter space of the MSUGRA model. We had investigated [9,13] several promising discovery channels that included

multi-jet $+\not\!E_T$ events (veto hard, isolated leptons) (J0L),

events with a single isolated lepton plus jets $+\not\!E_T$ (J1L),

events with two opposite sign isolated leptons plus jets $+\not\!E_T$ (JOS),

events with two same sign isolated leptons plus jets $+\not\!E_T$ (JSS),

events with three isolated leptons plus jets $+\not\!E_T$ (J3L),

events with two isolated leptons $+\not\!E_T$ (no jets, clean) (COS),

events with three isolated leptons $+\not\!E_T$ (with or without jets) (3L).

In these samples, the number of leptons is *exactly* that indicated, so that these samples are non-overlapping. For Tevatron data samples on the order of 0.1 fb^{-1}, the J0L signal generally gave the best reach for supersymmetry. It is the classic signature for detecting gluinos and squarks at hadron colliders. For larger data samples typical of those expected at the MI or TeV33, the clean 3L signal usually yielded the greatest reach except when leptonic decays of charginos and neutralinos are strongly suppressed — in this case, as we have already noted, the inclusive trilepton (3L) signal [15–17] with softer lepton cuts appears to provide the best strategy.[6] In the present paper, we will extend these results for models with non-universal GUT scale gaugino masses.

---

[5]Since the two lighter neutralinos contain significant Higgsino components, and $m_{\tilde{Z}_2} - m_{\tilde{Z}_1}$ is at least a few GeV for the **75** model (tens of GeV for the **200** model), we may expect LEP experiments might be able to detect signals from $e^+e^- \to \tilde{Z}_1\tilde{Z}_2$ production. For the **200** case, the non-observation of acollinear leptons or jets from $\tilde{Z}_2$ decay could lead to significant limits on its mass. In the **75** case the analysis will have to be redone since $m_{\tilde{Z}_2} - m_{\tilde{Z}_1}$ is just a few GeV, but it is worth keeping in mind that in the MSSM, ALEPH finds a mass bound of 79 GeV on $m_{\tilde{W}_1}$ that is derived by combining chargino and neutralino searches, assuming a mass gap ≥ 5 GeV. Finally, we note that in the **75** scenario, the branching fraction for the decay $\tilde{Z}_2 \to \tilde{W}_1 l \nu$ is significant; since the daughters of $\tilde{W}_1$ are likely to be soft, $\tilde{Z}_1\tilde{Z}_2$ production could result in ''monolepton'' events at LEP. While it is clear that a dedicated analysis is required to really exclude the ''hatched region'' for the **200**, and especially the **75** cases, we have chosen to show it using the same criteria in all four cases.

[6]This is not a subset of the J3L sample as there are additional cuts [16] to veto lepton pairs from W, Z, and (virtual) photons on this sample.
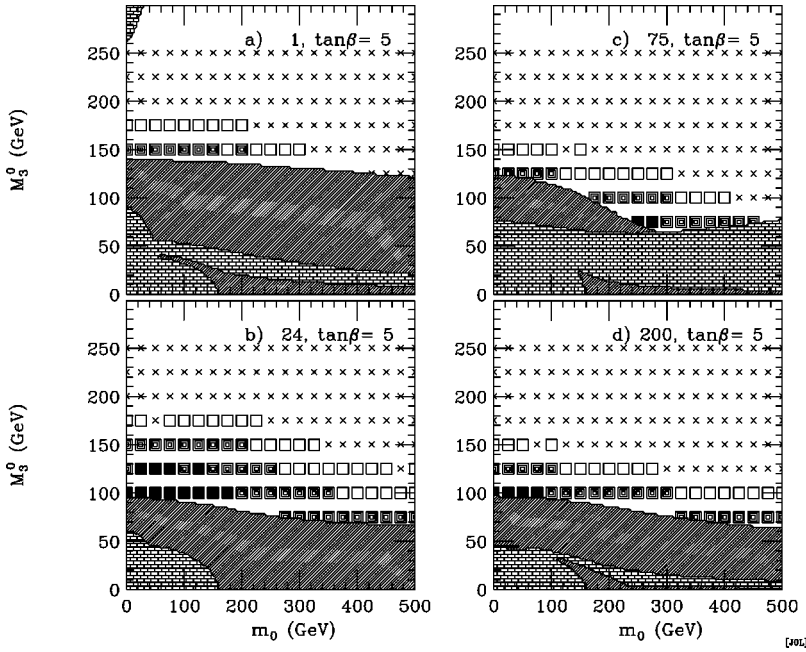
FIG. 6. A plot of parameter space points accessible to Fermilab Tevatron collider experiments with integrated luminosity 0.1 fb^{-1} (black squares), 2 fb^{-1} (gray squares) and 25 fb^{-1} (white squares) via the multijet$+\not{E}_T$ signal (J0L). Events containing isolated leptons have been vetoed. Points are plotted in the m_0 vs M_3^0 plane for SUGRA model parameters $A_0=0$, $\tan\beta=5$, and $\mu>0$ for the (a) $F_\Phi\sim1$, (b) $F_\Phi\sim24$, (c) $F_\Phi\sim75$, and (d) $F_\Phi\sim200$ models.

We have found that the second model described above with $F_\Phi\sim24$ can give rise to SUSY events at the Fermilab Tevatron which are rich in Z bosons. To extract this signal, we require identification of a leptonic "Z" boson ($Z\rightarrow e^+e^-$ or $\mu^+\mu^-$) plus jets plus $\not{E}_T$ (JZ).

To model the experimental conditions at the Tevatron, we use the toy calorimeter simulation package ISAPLT. We simulate calorimetry covering $-4<\eta<4$ with cell size $\Delta\eta\times\Delta\phi=0.1\times0.0872$. We take the hadronic (electromagnetic) energy resolution to be $70\%/\sqrt{E}$ ($15\%/\sqrt{E}$). Jets are defined as hadronic clusters with $E_T>15$ GeV within a cone with $\Delta R=\sqrt{\Delta\eta^2+\Delta\phi^2}=0.7$. We require that $|\eta_j|\leq3.5$. Muons and electrons are classified as isolated if they have $p_T>5$ GeV, $|\eta(l)|<2.5$, and the visible activity within a cone of $R=0.3$ about the lepton direction is less than $\max(E_T(l)/4,2$ GeV). In our analysis, we neglect multiple scattering effects, non-physics backgrounds from photon or jet misidentification, and make no attempt to simulate any particular detector explicitly.

We incorporate in our analysis the following trigger conditions: (1) one isolated lepton with $p_T(l)>15$ GeV and $\not{E}_T>15$ GeV, (2) $\not{E}_T>35$ GeV, (3) two isolated leptons each with $E_T>10$ GeV and $\not{E}_T>10$ GeV, (4) one isolated lepton with $E_T>10$ GeV plus at least one jet plus $\not{E}_T>15$ GeV, (5) at least four jets per event, each with $E_T>15$ GeV. Thus, every signal or background event must satisfy at least one of the above conditions. In addition to these basic selection and trigger criteria, we impose various additional cuts listed in Ref. [9] for all but the last of these channels where we use the soft SC2 cuts listed in Table I of Ref. [16]. For the jetty channels, we require $E_T(j_1)$, $E_T(j_2)$, and $\not{E}_T$ all to exceed a cut parameter E_T^c which is chosen to maximize the reach, while for the clean dilepton channel, we require rather hard leptons with $E_T(l_1,l_2)\geq(20,15)$ GeV.

We have generated the following physics background processes using ISAJET: $t\bar{t}$ production, $W+$jets, $Z+$jets,

WW, WZ, and ZZ production and QCD (mainly from $b\bar{b}$ and $c\bar{c}$ production). Each background subprocess was generated with the hard scattering subprocess final state particles in p_T bins of 25–50 GeV, 50–100 GeV, 100–200 GeV, 200–400 GeV, and 400–600 GeV. The numerical background values we use are listed in Fig. 2 of Ref. [9] and in Table II of Ref. [16] (for the 3L channel), and will not be repeated here.

For the new JZ event channel, we require two opposite sign same flavor isolated leptons (e or μ) with $m(l\bar{l})$ within $M_Z\pm8$ GeV. We also require $n(\text{jets})\geq2$, $S_T\geq0.2$, and $\not{E}_T\geq40$ GeV. In this case, the background rate was found to be 13.6 fb, mostly coming from $t\bar{t}$, WZ, and ZZ production.

IV. TEVATRON REACH RESULTS FOR SUGRA MODELS WITH NON-UNIVERSAL GAUGINO MASSES

In Figs. 6–21, we show the results of our computation of the SUSY reach of Tevatron collider experiments for models with non-universal gaugino masses. For each set of model input parameters, and for a given integrated luminosity, we consider a signal to be observable above background if (for some value of the cut parameter E_T^c for the jetty channels other than the JZ channel) $S>5\sqrt{B}$, $S>0.2B$, and $S>5$ (10) for integrated luminosity equal to 0.1 or 2 fb^{-1} (25 fb^{-1}), where S is the expected number of signal events and B is the expected number of background events. Within our framework, the scale of sparticle masses (and hence their production rates) is mainly determined by the parameters m_0 and M_3^0 (which fixes other gaugino masses at the unification scale). For this reason, the $m_0-M_3^0$ plane provides a convenient way to present our results. The results are somewhat less sensitive to variation of other parameters. In our analysis, we fix $A_0=0$ and choose $\mu>0$ (negative values of μ frequently do not yield the correct symmetry breaking pat-
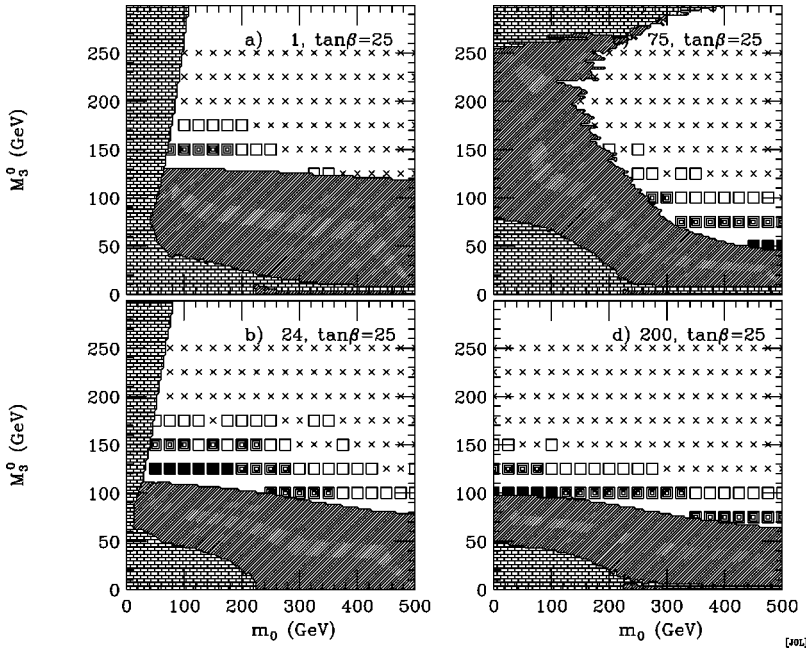
FIG. 7. The same as Fig. 6, except for $\tan\beta = 25$.

tern), and illustrate our results for $\tan\beta = 5$ and 25. Sampled points for which there is an observable signal for integrated luminosity of 0.1 fb^{-1} are denoted by black squares; gray squares denote points where the signal is observable with 2 fb^{-1}; and white squares, points that can be accessed with 25 fb^{-1}. Sampled points not accessible with even 25 fb^{-1} of integrated luminosity are denoted with an $\times$.

A. Reach via the J0L channel

Figure 6 shows results in the m_0 vs M_3^0 plane for $\tan\beta = 5$, $A_0 = 0$, and $\mu > 0$. These results are in the J0L channel, which is the classic signature for supersymmetry at hadron colliders. For the $F_\Phi \sim 1$ case with universal gaugino masses

in frame (a), we find no reach for MSUGRA (black squares) with the current Tevatron data sample beyond the region already excluded at LEP2. However, experiments at the MI should be able to probe M_3^0 values up to 150 GeV ($m_{\tilde{g}} \simeq 400$ GeV) for lower values of m_0. The TeV33 integrated luminosity extends this reach to $M_3^0 = 175$ GeV, corresponding to $m_{\tilde{g}} \simeq 480$ GeV. For the $F_\Phi \sim 24$ model in frame (b), there is a significant reach of *current* Tevatron experiments beyond the reach of LEP2. This is due mainly to the increased values of $m_{\tilde{W}_1}$ and $m_{\tilde{Z}_2}$ relative to their MSUGRA counterparts for a given value of M_3^0, so that just beyond the LEP2 limit, relatively light values of $m_{\tilde{g}} \sim 300$ GeV are still allowed, and can give rise to large J0L signals. The overall reach for SUSY in frame (b) extends to $M_3^0 = 175$ GeV,
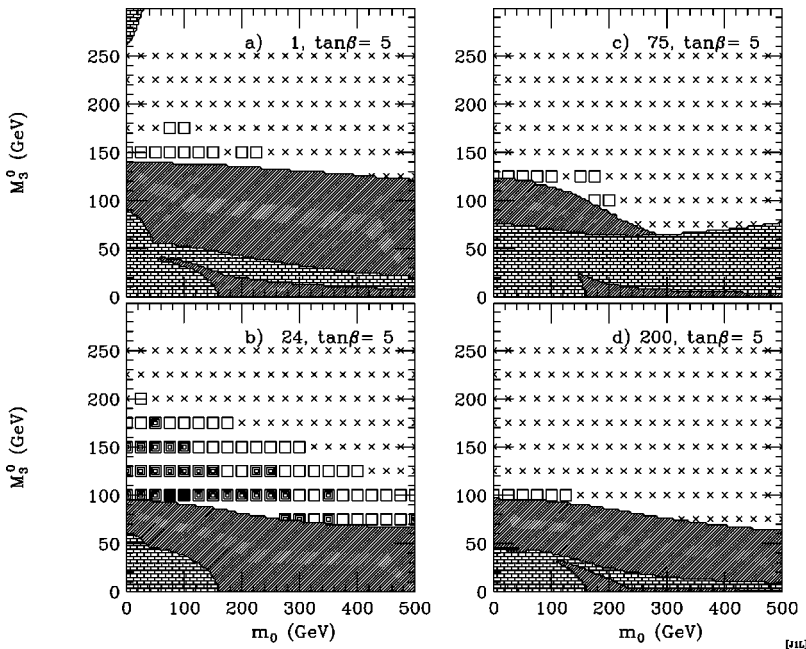
FIG. 8. The same as Fig. 6, except for the J1L signal.
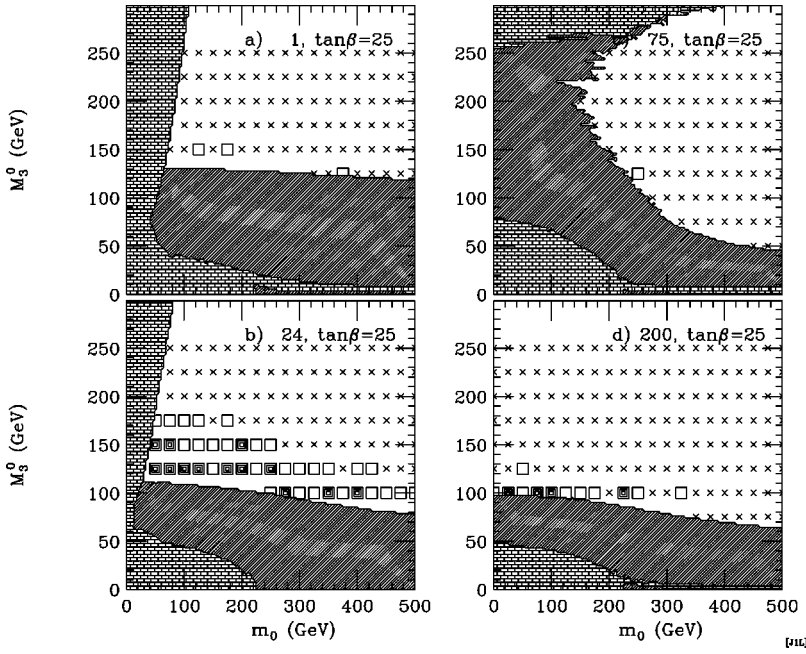
FIG. 9. The same as Fig. 7, except for the J1L signal.

which is comparable to the MSUGRA case in frame (a). For these large values of M_3^0, gluinos and squarks are heavy, and chargino and neutralino production is the dominant SUSY mechanism. For $M_3^0 = 175$ GeV, $m_{\tilde{W}_1}$ is significantly heavier in the **24** model relative to the MSUGRA case: the accessibility of heavier charginos is presumably due to the larger mass gap between the chargino and the LSP, which should increase the efficiency for detecting J0L events. For the $F_\Phi \sim$ **75** model in frame (c), the limits from LEP2 are again suppressed compared to the MSUGRA case due to heavier values of $m_{\tilde{W}_1}$ for a given value of M_3^0. In this model, $m_{\tilde{W}_1} \simeq m_{\tilde{Z}_1}$ so that there is very little visible energy from $\tilde{W}_1$ decays, and they behave effectively like the $\tilde{Z}_1$ in the detec-

tor, i.e. they give missing energy. Gluino and squark pair production gives rise to a significant J0L signal for low values of M_3^0, so that there is still a substantial reach for SUSY via the MI and TeV33. The reach of TeV33 is somewhat smaller than in the MSUGRA case because for values of $M_3^0 \simeq 175$ GeV, direct $\tilde{W}_1$ and $\tilde{Z}_2$ production dominates $\tilde{g}\tilde{g}$ and $\tilde{g}\tilde{q}$ production: e.g. for MSUGRA, $\tilde{W}_1\bar{\tilde{W}}_1$ production leads to jets$+\not{E}_T$ events, but for the $F_\Phi \sim$ **75** model no hard jets get produced in $\tilde{W}_1$ decay. Finally, the reach for the $F_\Phi \sim$ **200** model is shown in frame (d). In this model, as in the **75** case, relatively light values of $m_{\tilde{g}}$ are accessible to Tevatron experiments, and there is a significant reach for SUSY via the J0L signal. The black squares in the lower left of the frame come mainly from $\tilde{t}_1\tilde{t}_1$ and $\tilde{g}\tilde{g}$ events where
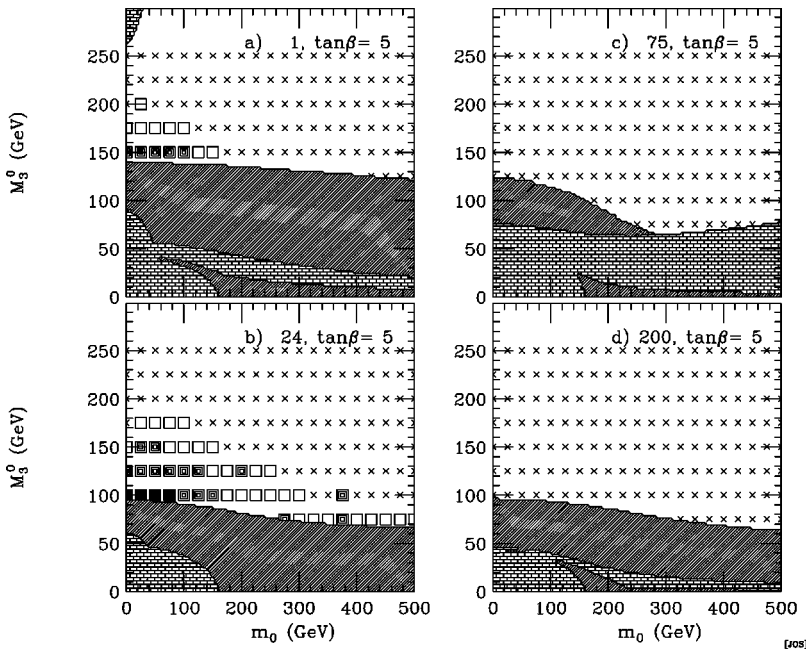
FIG. 10. The same as Fig. 6, except for the JOS signal.
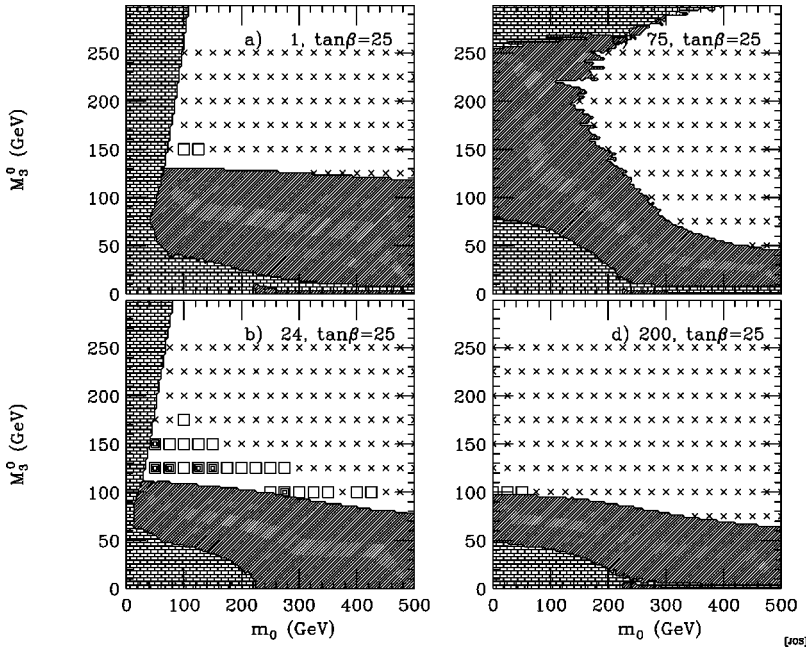
FIG. 11. The same as Fig. 7, except for the JOS signal.

$\tilde{g} \rightarrow b\tilde{b}_1$, so that the events are rich in b-jets. The ultimate reach of TeV33 again extends to $M_3^0 = 150$ GeV for low m_0, for which $m_{\tilde{g}} \simeq 400$ GeV.

Similar results for the reach of the Tevatron via the J0L channel are shown in Fig. 7 for $\tan\beta = 25$ (all other parameters are the same). The reach is somewhat diminished from the lower $\tan\beta$ case for all four models. Nevertheless, we see that there is significant reach via the Tevatron upgrades for supersymmetry in all models via the classic J0L channel.

B. Reach via the J1L channel

In Fig. 8 we show the Tevatron reach via the J1L signal for $\tan\beta = 5$. For the MSUGRA case in frame (a), there is no reach via the MI beyond the bounds from LEP2, but the TeV33 upgrade can access M_3^0 values as high as ~ 175 GeV for some parameter space points. For the $F_\Phi \sim \mathbf{24}$ model in frame (b), the Tevatron MI has considerable reach for SUSY via the J1L channel beyond the LEP2 bounds. Much of the reach at lower M_3^0 values comes from gluino and squark cascade decays to $\tilde{W}_1$ which then decays leptonically. The large mass gap between $\tilde{W}_1$ and $\tilde{Z}_1$ (shown in Fig. 3) results in a very energetic lepton which has a high probability for detection. TeV33 can access points with $M_3^0 \simeq 175$–200 GeV, corresponding to $m_{\tilde{g}} \sim 500$ GeV. When we next examine the reach in the $F_\Phi \sim \mathbf{75}$ and $F_\Phi \sim \mathbf{200}$ models in frames (c) and (d), we see no reach via the MI, and only a marginal
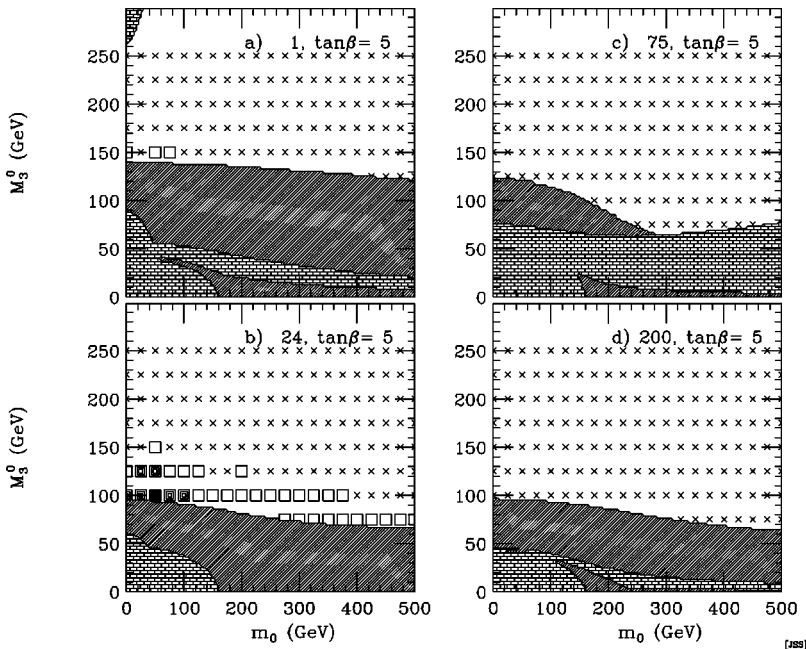
FIG. 12. The same as Fig. 6, except for the JSS signal.
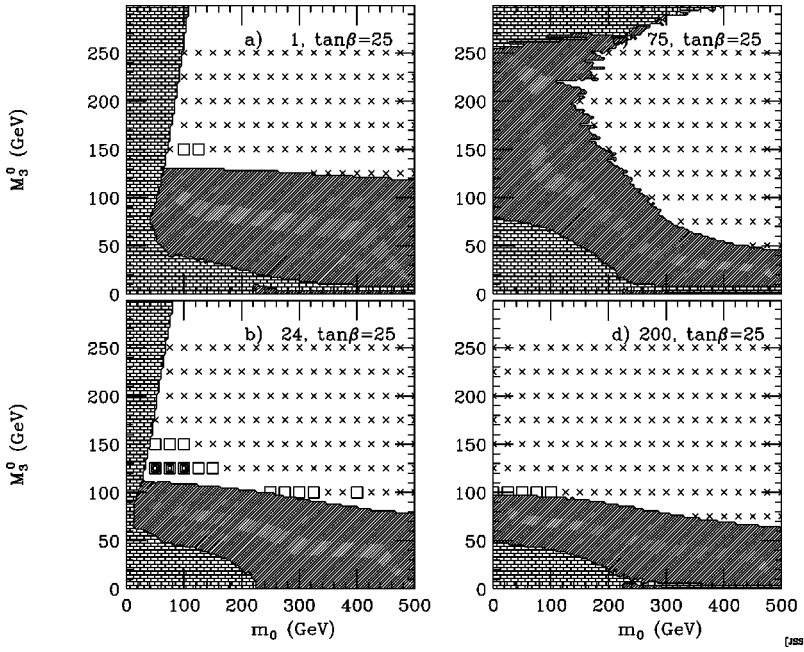
FIG. 13. The same as Fig. 7, except for the JSS signal.

reach via TeV33. Much of the signal presumably comes from cascade decays to $\widetilde{Z}_3$ for which the branching fraction is substantial—the $\widetilde{Z}_3$ can then decay into real vector bosons to give the leptonic signal. In these cases, the small mass gap between $\widetilde{W}_1$ and $\widetilde{Z}_1$ yields low energy leptons with a poor probability to pass cuts in the J1L channel, and furthermore, cascade decays to these states tend to be somewhat suppressed.

For the $\tan\beta = 25$ case in Fig. 9, in almost all the models, the reach via the J1L signal is diminished with respect to the lower $\tan\beta$ cases. Again, this is generally because at high $\tan\beta$, decays to b's and τ's are enhanced relative to decays into e's and μ's, making SUSY detection via leptonic modes in general more difficult. The exception here occurs with the

$F_\Phi \sim \mathbf{200}$ model, where there is some reach for the MI beyond the LEP2 bounds. In this case, some of the J1L events come from cascade decays involving $\widetilde{Z}_3$ which can decay via $\widetilde{Z}_3 \rightarrow \widetilde{W}_1 W$, and a hard lepton results from the W decay.

C. Reach via the JOS channel

The Tevatron reach via the JOS channel is illustrated in Figs. 10 and 11. For the MSUGRA case in frame (a) of Fig. 10, there is some reach by the MI and TeV33 for low values of m_0 where sleptons become relatively light, and charginos and neutralinos can directly decay to sleptons and sneutrinos. The isolated dileptons come from a variety of cascade decay mechanisms involving charginos, neutralinos, sleptons and sneutrinos. For the $F_\Phi \sim \mathbf{24}$ model in frame (b), there is a
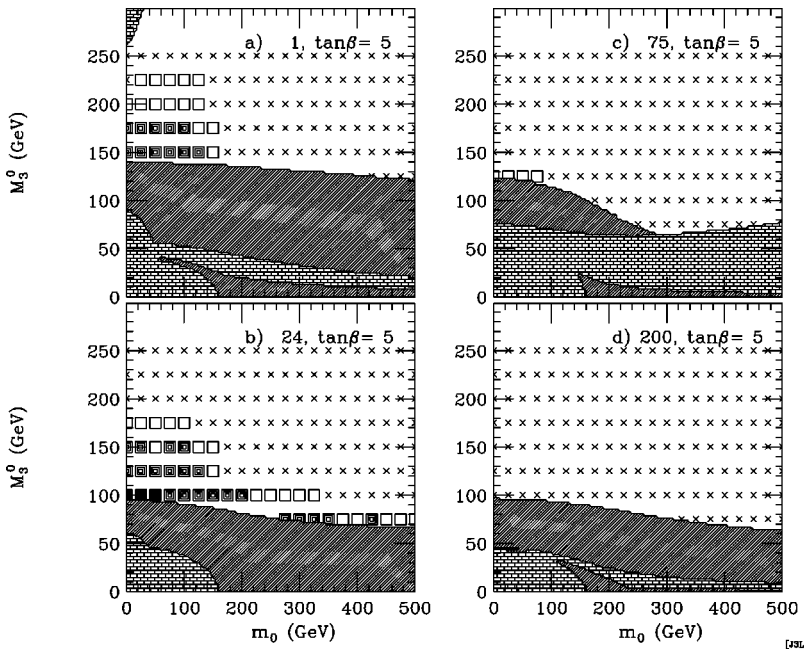
FIG. 14. The same as Fig. 6, except for the J3L signal.
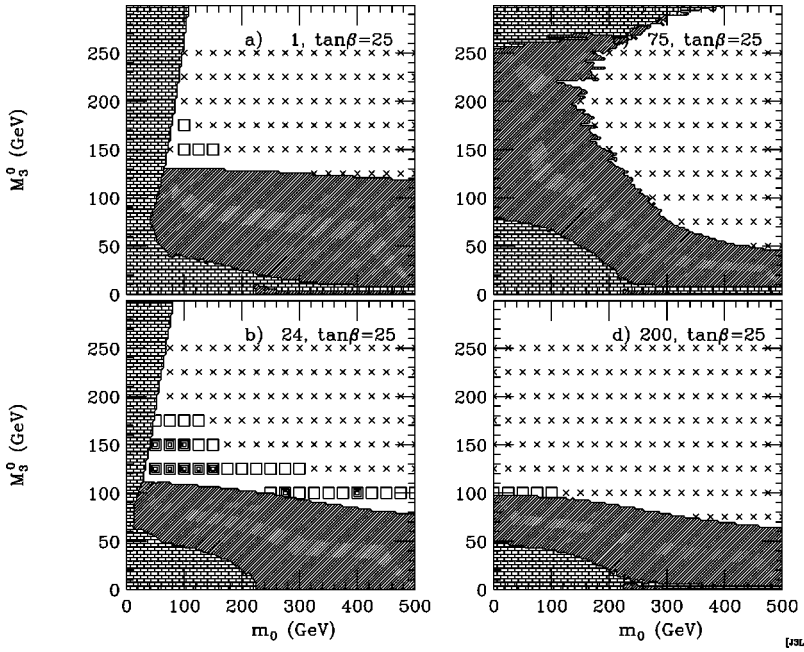
FIG. 15. The same as Fig. 7, except for the J3L signal.

significant reach by Tevatron experiments beyond the LEP2 bounds even with the current data sample, and the reach expands considerably for the MI and TeV33. The opposite sign (OS) dileptons again come from a variety of cascade decay mechanisms which include contributions from heavier charginos and neutralinos $\widetilde{W}_2$ and $\widetilde{Z}_3$. In the $F_\Phi \sim$ **75** and **200** models, there is *no reach* beyond the LEP2 bounds for any Tevatron luminosity upgrade in this channel. This is, per-

haps, not surprising if indeed the decays $\widetilde{Z}_3 \rightarrow W \widetilde{W}_1$ are the main source of J1L events, since the $\widetilde{W}_1$ is mostly invisible; i.e. any JOS event is doubly suppressed by the branching fraction of the cascade decay of gluino or squark into a lepton. We see a similar pattern for the $\tan \beta = 25$ case shown in Fig. 11, except also that the reach in the MSUGRA and $F_\Phi \sim$ **24** models is diminished due to the enhancement of decays to τ-leptons and b-quarks.
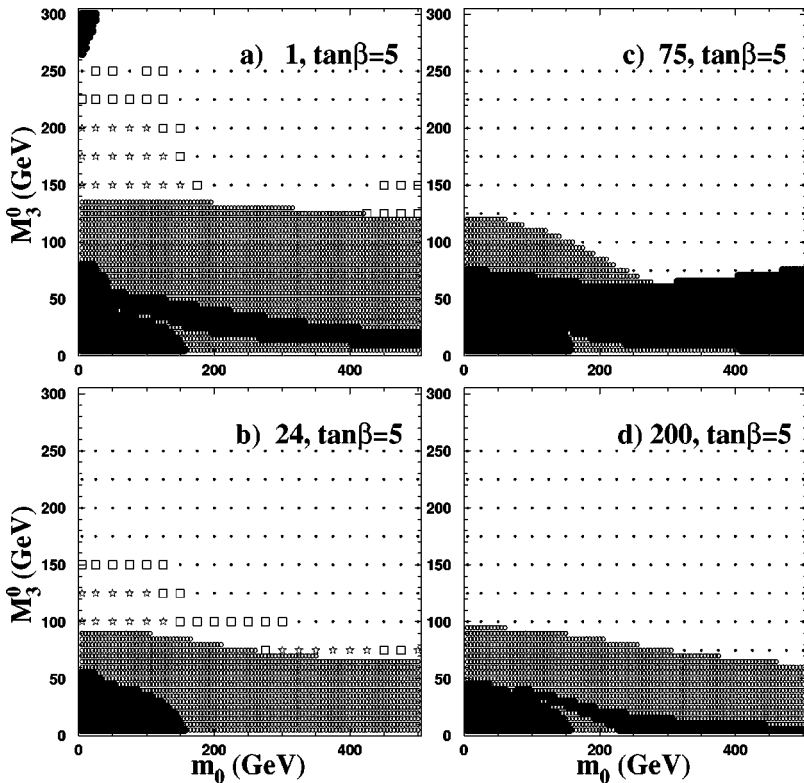
FIG. 16. The same as Fig. 6, except for the 3L signal. The stars denote the points (previously denoted by gray squares) where the signal is accessible at the MI.
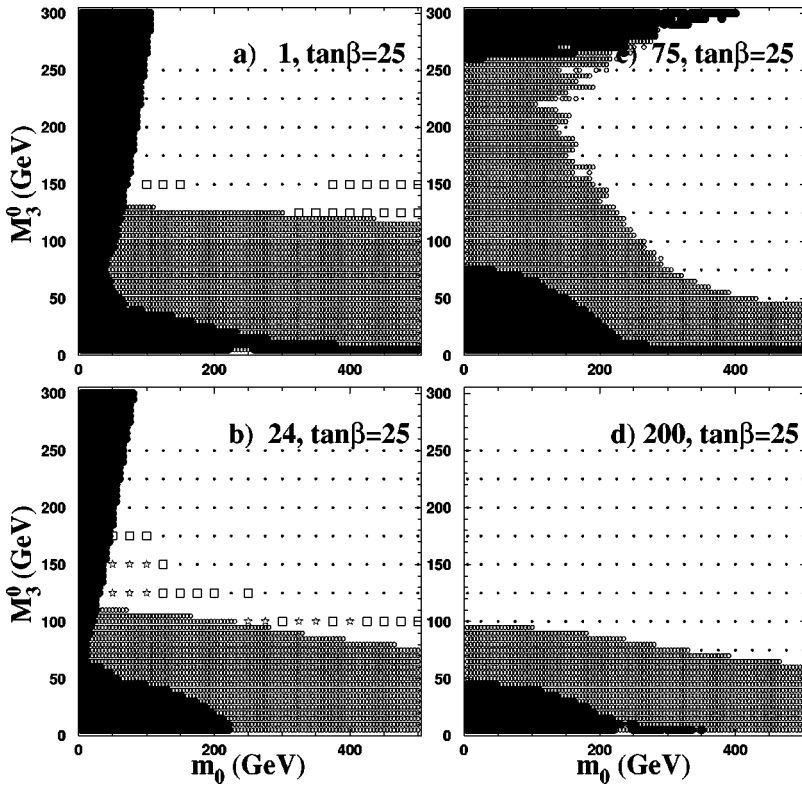
FIG. 17. The same as Fig. 16, except for $\tan\beta = 25$.

D. Reach via the JSS channel

The reach for SUSY in the JSS channel arises from the distinctive same-sign dilepton signal from cascade decays of the $\widetilde{g}$ to $\widetilde{W}_1$, where because of the Majorana nature of the gluino there is equal likelihood for same-sign and opposite-sign dilepton events. In the MSUGRA model in Fig. 12(a), there is only a tiny region that can be probed at the Tevatron in this channel mainly because the LEP2 bounds force $m_{\widetilde{g}}$ and $m_{\widetilde{q}}$ to such high values that their production cross sec-

tion is suppressed relative to direct chargino, neutralino and slepton pair production. For the $F_\Phi \sim \mathbf{24}$ model, however, lighter values of $m_{\widetilde{g}}$ are allowed beyond the LEP2 exclusion region, and furthermore, the large $\widetilde{W}_1$-$\widetilde{Z}_1$ decay gap gives rise to a relatively high probability to detect $\widetilde{g} \to \widetilde{W}_1 \to l$ cascade decay leptons. Consequently, we see a significant reach in the JSS channel in frame (b). Nonetheless, the reach is somewhat smaller than in the JOS channel, which also receives significant contributions from leptonic decays of neu-
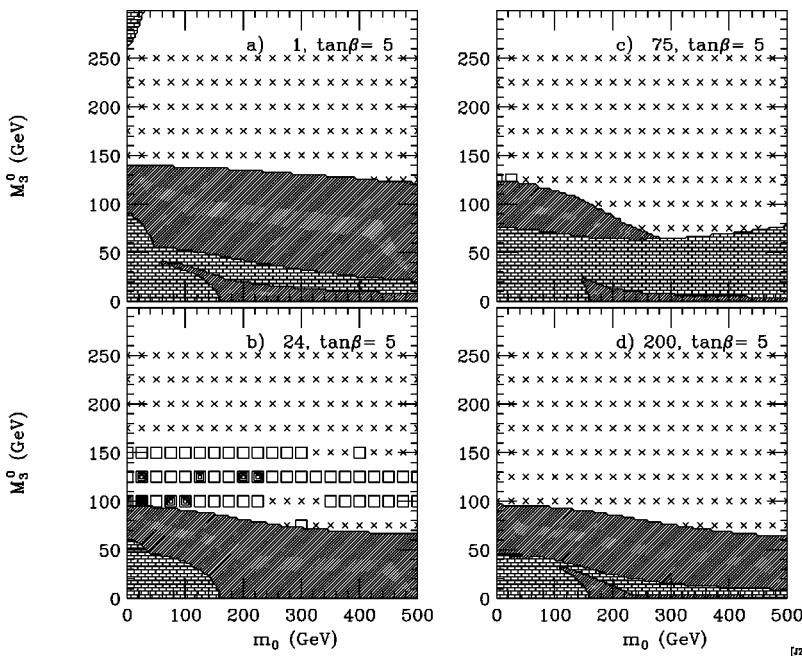
FIG. 18. The same as Fig. 6, except for the JZ signal.
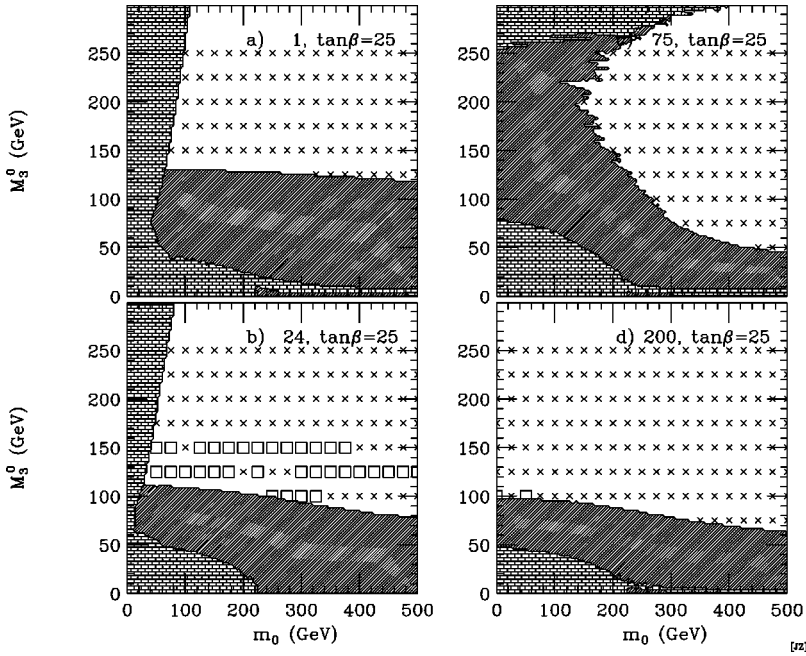
FIG. 19. The same as Fig. 7, except for the JZ signal.

tralinos. In the $F_\Phi \sim$ **75** and **200** models, there appears to be no signal in the JSS channel beyond the LEP2 region for much the same reasons that we just discussed for the JOS case. Broadly similar results hold for the $\tan\beta = 25$ case illustrated in Fig. 13, where we see the usual reduction in the region where there is an observable signal in the MSUGRA and in the $F_\Phi \sim$ **24** models.

E. Reach via the J3L channel

In Fig. 14, we show the reach of Tevatron experiments in the J3L channel. There is a significant reach by the Tevatron MI and TeV33 for MSUGRA for $m_0 \lesssim 150$ GeV extending all the way to $M_3^0 = 225$ GeV, corresponding to $m_{\tilde{g}} \simeq 600$ GeV, as shown in frame (a). The MSUGRA J3L signal dominantly comes from direct chargino, neutralino, slepton and sneutrino production and decays. In the $F_\Phi \sim$ **24** model, there is a significant reach in the J3L channel even
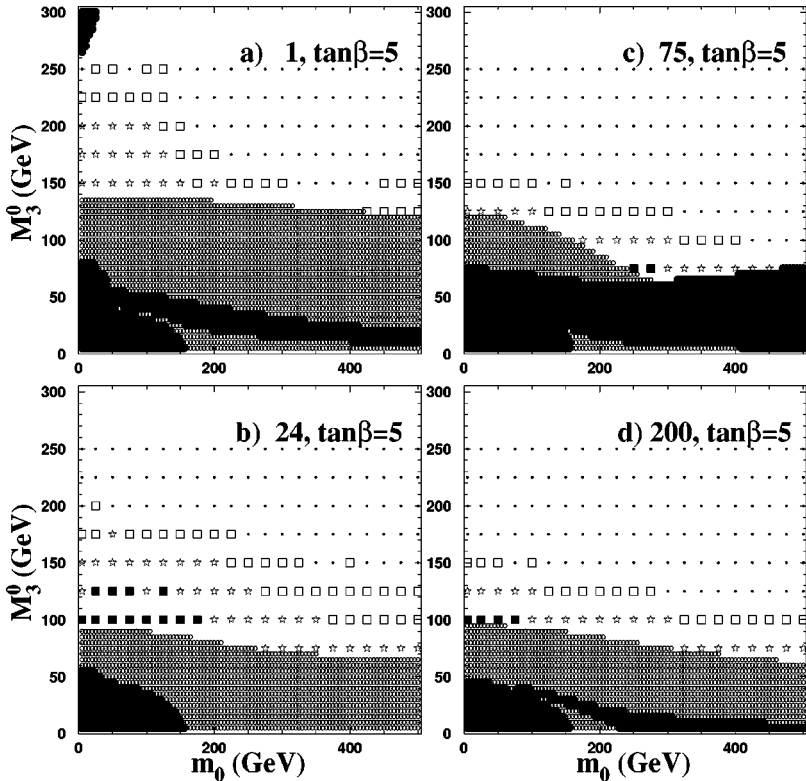
FIG. 20. The same as Fig. 6, except the reach is plotted for SUGRA models via *any* of the signals considered in this paper. Again the stars denote points (previously denoted by squares) accessible at the MI upgrade.
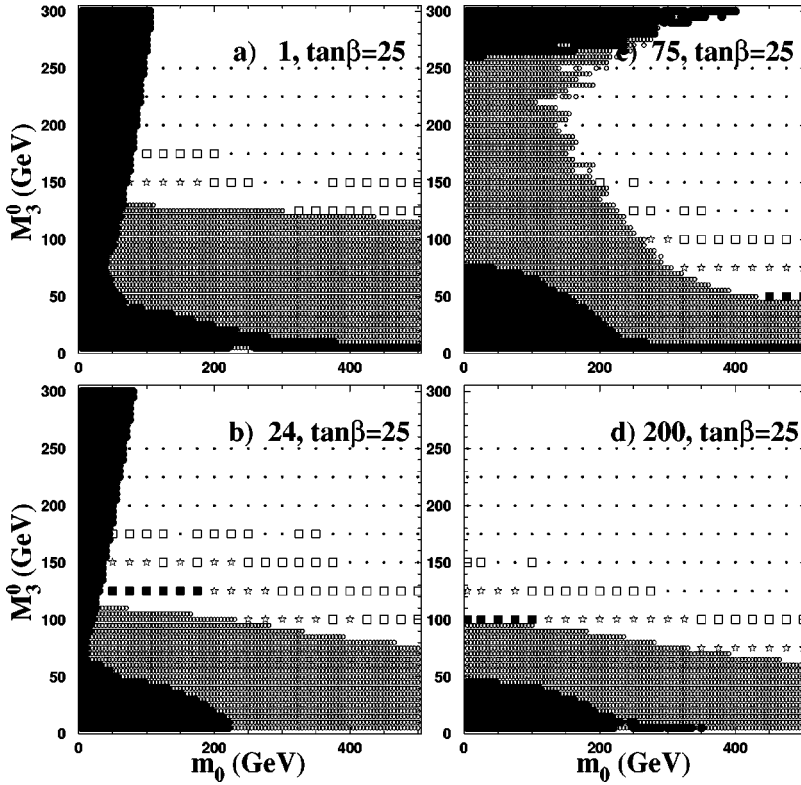
FIG. 21. The same as Fig. 20, except for $\tan \beta = 25$.

for large values of m_0 since $m_{\tilde{g}}$ can be as light as $\simeq 230$ GeV just beyond the LEP2 bound. For the largest values of M_3^0 where there is an observable signal in the MSUGRA and **24** cases, sparticle production is dominated by chargino and neutralino production, and the signal dominantly comes from $\tilde{W}_1 \tilde{Z}_2$ production with jets coming from QCD radiation. Because we only require leptons to have $E_T(l) \geqslant 10$ GeV, we expect that the efficiency increases by a relatively small amount despite the increase in $m_{\tilde{W}_1} - m_{\tilde{Z}_1}$ in going from the MSUGRA to the **24** case (in contrast to the case of the J0L signal where the increase in efficiency might be substantial). As a result the boundary of the TeV33 region occurs for similar values of $m_{\tilde{W}_1} \sim 170-180$ GeV. For the $F_\Phi \sim $ **75** and **200** models, there is again hardly any reach for SUSY in the J3L channel. For the large $\tan \beta = 25$ case illustrated in Fig. 15, the reach for all models in the J3L channel is diminished due to enhanced decays to 3rd generation particles, but for the **24** case, there is still a significant region beyond the current LEP reach that can be probed at Tevatron upgrades.

F. Reach via the 3L channel

The clean trilepton signal which often comes from $\tilde{W}_1 \tilde{Z}_2 \to 3l + \not{E}_T$ has frequently been considered the most promising signal via which to search for SUSY at luminosity upgrades of the Tevatron. These analyses have mainly been performed within the MSUGRA model. But even in this case, it has been known for some time that there are parameter space regions where there is no observable signal in this channel because chargino and neutralino decays to leptons may be suppressed. Our computation of the reach in this 3L

channel is shown in Fig. 16 for $\tan \beta = 5$. The stars denote the regions where there is an observable signal at the MI. For the MSUGRA model, the reach of the MI extends to $M_3^0 = 200$ GeV, while the TeV33 reach extends to $M_3^0 = 250$ GeV, corresponding to $m_{\tilde{g}} \simeq 650$ GeV. The well known gap in the reach at $m_0 \simeq 200-400$ GeV due to destructive interference in neutralino leptonic decays is clearly visible. There is substantial reach for SUSY in the $F_\Phi \sim $ **24** model both at the MI and TeV33. The reach in M_3^0 at low m_0 is, however, diminished relative to the MSUGRA model. This is because the large mass gap between $m_{\tilde{Z}_2}$ and $m_{\tilde{Z}_1}$ allows the spoiler decay modes $\tilde{Z}_2 \to Z \tilde{Z}_1$ and $\tilde{Z}_2 \to h \tilde{Z}_1$ to turn on at lower values of M_3^0. It is, however, interesting to see that there is an observable signal beyond the LEP bounds, for *all* values of m_0 scanned in the figure. For the $F_\Phi \sim $ **75** and **200** models, there is no reach for SUSY in the 3L channel, which underscores the model dependence of the much touted 3L signal. It may be of interest to examine whether the use of softer cuts [15] on the leptons affects this conclusion.

In the large $\tan \beta = 25$ case of Fig. 17, the MSUGRA reach is diminished at low m_0 due to enhanced decays to τ leptons. There remains a significant reach for SUSY in the 3L channel for the $F_\Phi \sim $ **24** model at large $\tan \beta$ because the large mass gap between $m_{\tilde{Z}_2}$ and $m_{\tilde{Z}_1}$ allows $\tilde{Z}_2$ decays to real selectrons and smuons to compete with decays to staus.

We have also checked the reach via the COS channel. While there are parameter regions where this could provide confirmation of a signal in other channels, the COS topology does not appear to increase the reach beyond what is observable via other channels.

G. Reach via the JZ channel

It is possible to produce real Z bosons in SUSY particle cascade decay events. Events with an identified Z boson plus $\not{E}_T$ are interesting because standard model backgrounds to these mainly come from vector boson pair production or $t\bar{t}$ production where the leptons from the decays of the tops accidentally reconstruct the Z mass, and hence, are small. Prospects for observing just this signal at the Tevatron collider were examined long ago in the context of the MSSM framework [24]. In this study, the focus was on relatively small values of μ and $m_{\tilde{g}}$, so that all the charginos and neutralinos were accessible via the production and subsequent decays of gluinos.

Although JZ events are possible within the MSUGRA framework, they typically occur at very low rates, at least for sparticle masses accessible at the Tevatron. To understand this, we first recall that because $|\mu| \gg M_1$, M_2 as is typical in MSUGRA, the lighter neutralinos and the lighter chargino are mainly gaugino-like, while the heavier ones are Higgsino-like. But since the Z boson couples only to Higgsino pairs or charged gaugino pairs, it is clear that the widths for the decays $\tilde{Z}_{3,4} \to \tilde{Z}_{1,2}Z$ or $\tilde{W}_2 \to \tilde{W}_1 Z$ are suppressed by gaugino-Higgsino mixing angles.

Our results for the observability of SUSY events in the JZ channel are shown in Fig. 18 for $\tan\beta = 5$, and in Fig. 19 for $\tan\beta = 25$. Indeed we see from Fig. 18(a) that there is *no reach* at either the Tevatron MI or TeV33 for MSUGRA in the JZ channel. However, for the $F_\Phi \sim \mathbf{24}$ model, in frame (b) $|\mu| \sim M_2$, and the $\tilde{Z}_3$ can be light enough that it can be directly produced in collider events, while its decay branching fraction to Z is substantial: ~ 10–50%. Also, the large $\tilde{Z}_2 - \tilde{Z}_1$ mass gap allows the decay $\tilde{Z}_2 \to Z\tilde{Z}_1$ to occur (via the subdominant Higgsino component of $\tilde{Z}_1$) in much of parameter space. We see in Fig. 18(b) that while this signal might be detectable at the MI for a limited range of parameters, the reach of TeV33 in this channel is indeed substantial, covering much of parameter space below $M_3^0 \lesssim 150$ GeV. Meanwhile, for the $F_\Phi \sim \mathbf{75}$ and $\mathbf{200}$ models, there is again no reach for SUSY in the JZ channel—the branching fractions for cascade decays to heavier neutralinos and charginos tend to be small in these cases.

For the $\tan\beta = 25$ case in Fig. 19, there is again no reach for SUSY in the MSUGRA model or the $F_\Phi \sim \mathbf{75}$ and $\mathbf{200}$ models. In the $F_\Phi \sim \mathbf{24}$ model, there is a significant Tevatron reach in the JZ channel, but only for TeV33 type integrated luminosities. Since the JZ signal occurs at an observable level only in rather special models, the observation of such a signal in tandem with more conventional SUSY signals would be especially interesting since it could stringently restrict the underlying framework.

V. SUMMARY AND CONCLUDING REMARKS

The search for SUSY has become a standard item on all high energy physics experiments searching for physics beyond the standard model. For the most part, the analyses of current experiments as well as projections of capabilities of future experiments have been carried out within the framework of the MSUGRA model, or within the MSSM framework with some *ad hoc* assumptions motivated by MSUGRA about scalar and gaugino masses. Since SUSY cross sections, after experimental cuts, are expected to be sensitive to sparticle mass and mixing patterns (which are determined by the presently unknown dynamics of SUSY breaking), it is worthwhile to examine just how much the SUSY reach of future facilities changes in alternative scenarios.

These considerations motivated us to examine SUSY signals at Tevatron upgrades in the supergravity $SU(5)$ model [8] with non-universal gaugino masses at the GUT scale. For simplicity, other parameters were considered to unify as in the MSUGRA model. Such a scenario can be realized if there is a superfield Φ that is charged under $SU(5)$ and whose auxiliary component develops a VEV that breaks the GUT gauge group down to the standard model gauge group. The resulting GUT scale gaugino masses are determined by the transformation properties of Φ, which can transform as the **1** (this corresponds to MSUGRA), **24**, **75** or the **200** dimensional representation of $SU(5)$. The resulting gaugino mass ratios at the GUT scale along with their renormalized values at the weak scale (relevant for phenomenology) are shown in Table I. The phenomenology is altered not only because of the differences in these weak scale gaugino masses, but also because the difference in the boundary condition on gaugino masses alters the renormalization group evolution of other parameters as well.

Our main result is the reach of Tevatron Main Injector and its possible TeV33 luminosity upgrade for the cases where Φ belongs to any one of these irreducible representations. We have examined this reach for various event topologies. The results of our calculation are shown in Figs. 6–19. The cumulative reach for SUSY, i.e. the region of the $m_0 - M_3^0$ plane where there should be an observable signal in at least one of the channels, is shown in Figs. 20 and 21. The precise reach is model-dependent. In Fig. 20(a), the reach in the MSUGRA model is built entirely out of the reach in the J0L and 3L channels. For some of the points examined, there may be observable signals in other channels as well. The reach of the Tevatron for the $F_\Phi \sim \mathbf{24}$ model is built out of the J0L, J1L and JZ channels, i.e., for a few points the SUSY signal appears to be observable only via the JZ channel, and not in the more standard J0L and 3L channels. In addition, over much of the observable parameter space, signals should also be detectable in many different leptonic channels. The additional signals should help in constraining the underlying model. In contrast, the reach in the **75** and **200** models shown in Fig. 20(c) and (d), the cumulative reach plot coincides with the reach plot for the J0L channel (Fig. 6). In fact, the leptonic signals for SUSY will be observable for only extremely restricted regions of model parameters. This underscores the importance of the J0L channel in that it is relatively model independent, at least so long as the LSP is a stable neutralino which escapes detection: experimentalists should scrutinize this channel closely even if no leptonic SUSY signals can be seen. We should also mention that in our analysis, we have not attempted to really optimize the

reach in this channel. By judiciously choosing the cuts, it may be possible to increase the reach somewhat beyond what appears in the figure.

For the $\tan\beta = 25$ case shown in Fig. 21, the cumulative reach for MSUGRA shown in frame (a) is again defined by just the J0L and 3L channels but is somewhat reduced relative to the corresponding low $\tan\beta$ case. The reach for the $F_\Phi \sim$ **24** model shown in frame (b) is defined by just the J0L and JZ channels, which underscores the importance of an independent search for SUSY in the JZ channel. The reach is only slightly diminished from the $\tan\beta = 5$ case. The Tevatron SUSY reach for the $F_\Phi \sim$ **75** and **200** models for $\tan\beta = 25$ is again defined solely by the J0L channel; very few of these parameter space points are accessible in any other channel. Thus, a SUSY discovery with a signal only in the J0L channel may indicate non-universal gaugino masses which act to suppress leptonic signals originating from SUSY particle cascade decays.

In summary, we have examined the SUSY reach of luminosity upgrades of the Tevatron in non-minimal SUGRA type models where gaugino masses are not unified at some high scale. We find that rates for various signal topologies (and hence, the reach) can be quite different from MSUGRA expectations. There may be new signatures such as the high $p_T Z + \not{E}_T$ signal in the **24** model that are unobservable in the MSUGRA picture. On the other hand, in the **75** and **200** models a signal might be observable only in the canonical multijet $+ \not{E}_T$ channel. This is in contrast to R-parity violating models [25] where there might be observable signals *only* in the multilepton channel, but no signal in the usual $\not{E}_T$ channel. We thus conclude that while it might well be possible to discover a signal for new physics at the Tevatron, its interpretation will have to be done with care. What we do not see, in addition of course to what we do see, may play an important role in unravelling the nature of the new physics.

Note added. In the analysis of inclusive trilepton events reported here, we have included backgrounds from $W^*\gamma^*$ and W^*Z^* production that were ignored in the first version of this paper, but have recently been shown to be the main source of SM backgrounds [17,16,15].

[1] A. Chamseddine, R. Arnowitt, and P. Nath, Phys. Rev. Lett. **49**, 970 (1982); R. Barbieri, S. Ferrara, and C. Savoy, Phys. Lett. **119B**, 343 (1982); L. J. Hall, J. Lykken, and S. Weinberg, Phys. Rev. D **27**, 2359 (1983); for a review, see H. P. Nilles, Phys. Rep. **110**, 1 (1984).

[2] For recent reviews, see X. Tata, ''Lectures presented at the IX Jorge Swieca Summer School,'' Campos do Jordão, Brazil, 1997, UH-511-872-97, hep-ph/9706307; S. Dawson, Lectures at TASI 97, hep-ph/9712464, (1997).

[3] E. Cremmer, S. Ferrara, L. Girardello, and A. Van Proeyen, Phys. Lett. **116B**, 231 (1982).

[4] C. T. Hill, Phys. Lett. **135B**, 47 (1984).

[5] Q. Shafi and C. Wetterich, Phys. Rev. Lett. **52**, 875 (1984).

[6] J. Ellis, K. Enqvist, D. Nanopoulos, and K. Tamvakis, Phys. Lett. **155B**, 381 (1985).

[7] M. Drees, Phys. Lett. **158B**, 409 (1985).

[8] G. Anderson *et al.*, in *New Directions for High Energy Physics, Snowmass 96*, edited by D. G. Cassel, L. Trindle Gennari, and R. H. Siemann (Stanford Linear Accelerator Center, Menlo Park, CA, 1997); see also J. Amundson *et al.*, in *New Directions for High Energy Physics, Snowmass 96*, edited by D. G. Cassel, L. Trindle Gennari, and R. H. Siemann (Stanford Linear Accelerator Center, Menlo Park, CA, 1997).

[9] H. Baer, C-H. Chen, C. Kao, and X. Tata, Phys. Rev. D **52**, 1565 (1995); H. Baer, C-H. Chen, F. Paige, and X. Tata, *ibid.* **54**, 5866 (1996).

[10] S. Mrenna, G. Kane, G. Kribs, and J. Wells, Phys. Rev. D **53**, 1168 (1996).

[11] D. Amidei, *et al.*, ''Report of the TeV 2000 Working Group,'' Fermilab-Pub-96/082 (1996).

[12] S. Mrenna *et al.*, in *Proceedings of the 1996 Snowmass Summer Study*, edited by D. G. Cassel, L. Trindle Gennari, and R. H. Siemann (Stanford Linear Accelerator Center, Menlo Park, CA, 1997).

[13] H. Baer, C-H. Chen, M. Drees, F. Paige, and X. Tata, Phys. Rev. Lett. **79**, 986 (1997); Phys. Rev. D **58**, 075008 (1998).

[14] H. Baer, K. Hagiwara, and X. Tata, Phys. Rev. D **35**, 1598 (1987); R. Arnowitt and P. Nath, Mod. Phys. Lett. A **2**, 331 (1987); H. Baer and X. Tata, Phys. Rev. D **47**, 2739 (1993); H. Baer, C. Kao, and X. Tata, *ibid.* **48**, 5175 (1993); S. Mrenna, G. Kane, G. D. Kribs, and J. D. Wells, *ibid.* **53**, 1168 (1996).

[15] V. Barger, C. Kao, and T. Li, Phys. Lett. B **433**, 328 (1998); V. Barger and C. Kao, Phys. Rev. D **60**, 115015 (1999).

[16] H. Baer, M. Drees, F. Paige, P. Quintana, and X. Tata, FSU-HEP-990509, hep-ph/9906233 (1999).

[17] K. Matchev and D. Pierce, Phys. Rev. D **60**, 075004 (1999); Phys. Lett. B **467**, 225 (1999).

[18] F. Paige, S. Protopopescu, H. Baer, and X. Tata, hep-ph/9804321 (1998).

[19] N. Arkani-Hamed, H-C. Cheng, and T. Moroi, Phys. Lett. B **387**, 529 (1996).

[20] A. Brignole, L. Ibanez, and C. Munoz, Nucl. Phys. **B422**, 125 (1994), **B436**, 747; (E) (1995); A. Brignole, L. Ibanez, C. Munoz, and C. Scheich, Z. Phys. C **74**, 157 (1997).

[21] C. H. Chen, M. Drees, and J. Gunion, Phys. Rev. Lett. **76**, 2002 (1996); Phys. Rev. D **55**, 330 (1997).

[22] ALEPH Collaboration, R. Barate *et al.*, Eur. Phys. J. C **2**, 417 (1998).

[23] M. Hohlmann, Fermilab-Conf-96/330-E (1996).

[24] H. Baer, X. Tata, and J. Woodside, Phys. Rev. D **42**, 1450 (1990).

[25] H. Baer, C. Kao, and X. Tata, Phys. Rev. D **51**, 2180 (1995).